NANOSTRUCTURED SURFACES FOR DRAMATIC REDUCTION OF FLOW RESISTANCE IN DROPLET-BASED MICROFLUIDICS

Joonwon Kim and Chang-Jin "CJ" Kim

Mechanical and Aerospace Engineering Department, University of California, Los Angeles (UCLA)
Los Angeles, CA 90095, U.S.A.

ABSTRACT

This paper reports a dramatic reduction of liquid droplet flow resistance by engineering the surfaces into nanomechanical hydrophobic structures that shows the contact angle over 175°. Flow resistances of droplets on open surfaces as well as in confined microchannels (between surfaces) have been measured with significant reduction of flow resistance (over 99% and over 95%, respectively) compared with a surface of the same material.

INTRODUCTION

Fabrication and calibration of hydrophobic contacts have recently been reported with different methods of surface modifications [1-10]. The main idea of obtaining such a high contact angle is due to composite interface (hydrophobic structure and air) at the contact. Most of the hydrophobic surfaces with contact angle over 170° were obtained mainly by chemical treatment or modifying polymer surfaces [1-6]. It is important to note that, for our goal of reducing flow resistance, high contact angle surfaces do not necessarily mean the reduction, even at contact angle over 170°. In fact, the rough hydrophobic surface with insufficient scale of projections can decrease the area of trapped air under a droplet that increases the resistance against droplet sliding [2]. Both large contact angle and small contact angle hysteresis (proper scale of projections) should be considered for a surface with low resistance.

Typical applications for these hydrophobic surfaces are mentioned as self cleaning mechanism [10] and electrostatic actuation droplet on the hydrophobic surface [4]. However, the discussions have all been limited to open surfaces.

In this paper, we study reduction of flow resistance of droplets not only on open surface but also in channel configuration. Noting the severe flow resistance in microfludics, which results in high pressure drop in micropumping, our nanomechanical hydrophobic surface is being developed to minimize the problem.

Considering the requirements for the effective hydrophobic surface and additional features of our hydrophobic surface such as;

- Robust nano-size mechanical structure rather than chemically formed surface or roughened polymer surface contact.
- Selective modification of desired area by lithographical technique.
- Structure (silicon) can be used as an electrical material for other application

the concept and theory that bring about the dramatic decrease of flow resistance is discussed, and a series of systematic experiments are presented.

BASIC CONCEPT AND THEORY

Contact angle modification

By using classical Young's equation:

$$\cos\theta = \frac{\gamma_{sv} - \gamma_{ls}}{\gamma_{lv}} \qquad (1)$$

where γ_{lv}, γ_{sv}, and γ_{ls} are surface tensions at liquid/vapor, solid/vapor and liquid/solid interface, respectively, the contact angle θ of a liquid droplet on a flat homogeneous solid surface can be described.

However, the condition of contact surface can modify the apparent contact angle. Since the Young's equation only works with the flat homogeneous surface, other expanded approach is needed to describe contact angle of a droplet on rough surfaces that have composite interface at contact. Cassie and Baxter suggested a relationship that describes the apparent (averaged) contact angle of the droplet on the composite surface by following equation [11]:

$$\cos\theta' = f\cos\theta + (1-f)\cos\theta_1 \qquad (2)$$

where θ' is the apparent contact angle on composite surfaces, θ and θ_1 are the contact angle of the droplet on different surfaces, and f and (1-f) are unit area fractions of the different surface. For a rough surface with hydrophobic structure, Equation 2 can be expressed as following:

$$\cos\theta' = f\cos\theta + f - 1 = f(\cos\theta + 1) - 1 \qquad (3)$$

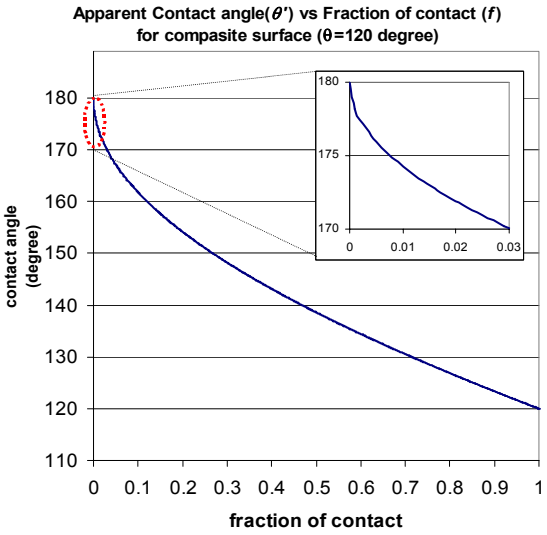

***Fig. 1**: Plot of apparent contact angle vs fraction of contact*

substituting 180° for θ_l since air is trapped among the hydrophobic structure and under the droplet.
Therefore, the apparent contact angle on a hydrophobic structure with a given fractional contact can be predicted. According to Equation 3, it is clear that θ' increases with smaller f. Fig.1 show this relationship with a given θ =120° (i.e. Teflon). So, in order to obtain higher contact angle, it is necessary to make smaller contact. For example, the fraction of contact needs to be smaller than 1% in order to get the apparent contact angle above 175° as shown in Fig.1.

Sliding angle

In general, a droplet with a higher contact angle gives smaller contact area (also means shorter contact line width of droplet) that causes low sliding resistance for the droplet movement. Contact angle hysteresis is also a key parameter to determine the sliding resistance. The sliding resistance is most conveniently tested by tilting experiment. Following relationship was carried out in [12] and [13], respectively:

$$\sin\alpha \propto \frac{r}{mg} \qquad (4)$$

$$\frac{mg\sin\alpha}{w} \propto (\cos\theta_{rec} - \cos\theta_{adv}) \qquad (5)$$

where α, r, w, and mg are sliding angle, radius of contact area, and gravitational force due to mass m. Also, θ_{rec} and θ_{adv} are receding and advancing angle that determine contact angle hysteresis. Even though specific forms of these relationships were used for flat surfaces, they can still be applied on composite surfaces.

SAMPLE FABRICATION PROCESS

The fabrication of micro/nanostructured samples is explained with Fig.2. In order to visualize droplet behavior from top, a transparent substrate (i.e. Borofloat™ glass) is used with a thin layer of silicon for viewing side (Fig. 2a) instead of just a silicon substrate (Fig. 2b). In Fig. 2a, a SOI wafer is anodically bonded on the transparent substrate facing thin (15μm) silicon side that becomes structured patterns. The thickness of 15μm is selected for testing to ensure "proper scale of projection" (respect to microstructure dimensions) that is explained in the previous section. After anodic bonding, the substrate is etched with KOH in order to remove unwanted silicon side from SOI wafer. KOH etching is then stopped at the exposed surface of a thermal oxide layer. In the following steps, the oxide layer is removed by BOE, and the thin silicon side is patterned by DRIE. In the same manner, a silicon wafer is also patterned. SEM pictures of the patterned structures are shown in Fig. 3a and Fig. 3b.

After DRIE, 0.2% of Teflon solution is spin-coated to form a layer of thickness around 200Å on the patterned structures. For channel configuration (Fig. 2c), Teflon spacers (thickness of 1mm) are used to separate the two surfaces.
However, since fabrication of nanostructures by such high-resolution lithography as E-beam writer is not economical and severely limits the area of patterns, an

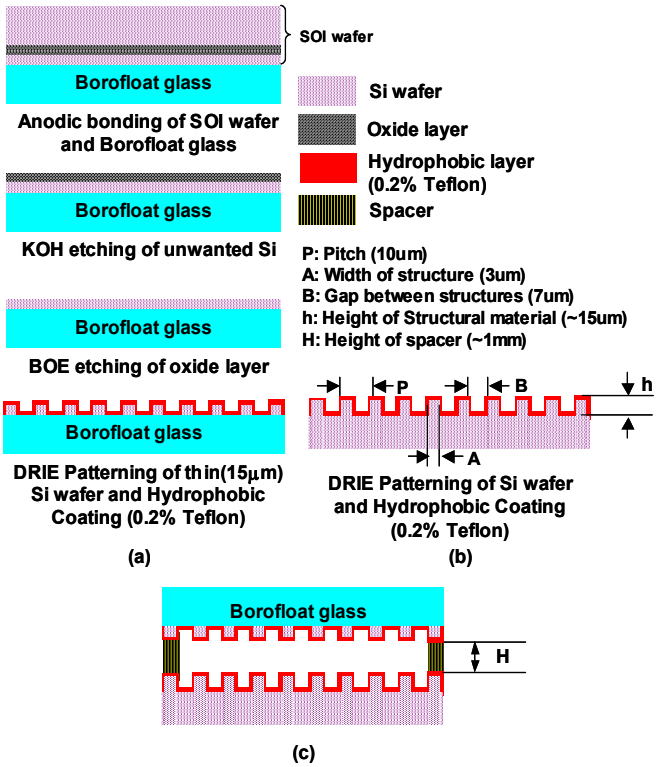

***Fig. 2**: Process flow of micropattern surface (a) with transparent substrate, (b) with silicon substrate, and (c) assembled channel.*

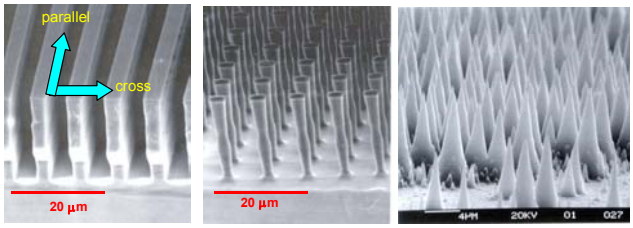

(a) (b) (c)

Fig. 3*: SEM pictures of structured hydrophobic surfaces. (a) Microline pattern, (b) Micropost pattern, and (c) Nanopost pattern.*

alternate way of generating effective nanostructured surfaces is considered. By controlling the process parameters of DRIE (similar way of silicon grass formation during fluorine–based RIE [14,15]), the effective nanostructured surfaces (sharp tip) are formed as shown in Fig. 3c. This method is used to utilize well-known problem (Black Silcon) during RIE into a useful tool to form our nanostructure.

EXPERIMENT

A total of five different surface layouts are tested including a flat surface as a reference surface, microline pattern with two different directions (Fig. 3a), micropost pattern and a nanostructured surface as an ultimate surface. The contact angles of each sample surface are measured in order to compare hydrophobicity (Fig. 4). The measured contact angles show good agreement with the graph shown in Fig. 1. Flow resistance of droplets is measured by the test schematically shown in Fig. 5. Simple tilting experiment is appropriate as we are interested in the relative resistance among different surfaces. The sliding angle α of each sample is measured with water droplets of four different volumes (12μl, 17μl, 22μl, and 27μl). For the channel configuration, the droplets are squeezed between two wafers that contain the same surface patterns and are held by 1mm thick spacers. In addition, since it is almost impossible to keep the water droplets stationary on the nanostructured surface against

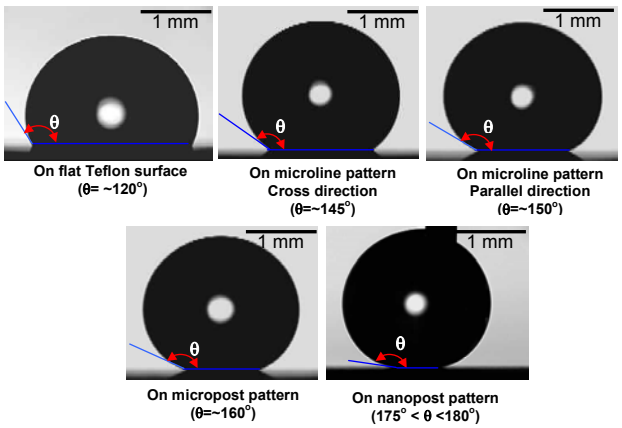

Fig. 4*: Contact angles of different hydrophobic surfaces. (droplet volume:~4μl)*

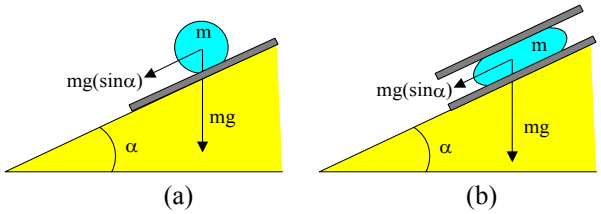

Fig. 5*: Schematic of angle measurement. (a) Open configuration and (b) Channel configuration.*

rolling, the nanostructures are formed on the recessed surface inside the KOH etched cavity (long rectangular area with a depth of 50μm).

RESULT AND DISCUSSION

Testing results of both open and channel configurations are plotted in Fig. 6, which expresses the flow resistance with the inclination angle that initiates the flow as a function of droplet size. Smaller droplets have more resistance against flowing down, as one can suspect from dominance of surface tension effect over mass effect. Reduction of flow resistance on structured surfaces is clear when the values of sin(α) are compared among different surfaces for a given droplet volume. In the case of open configuration with the nanostructured surface, the

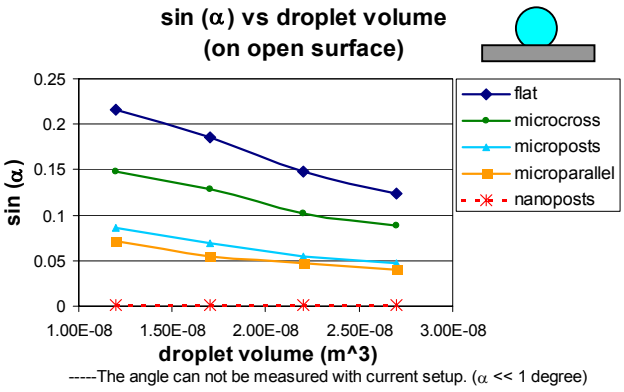

(a)

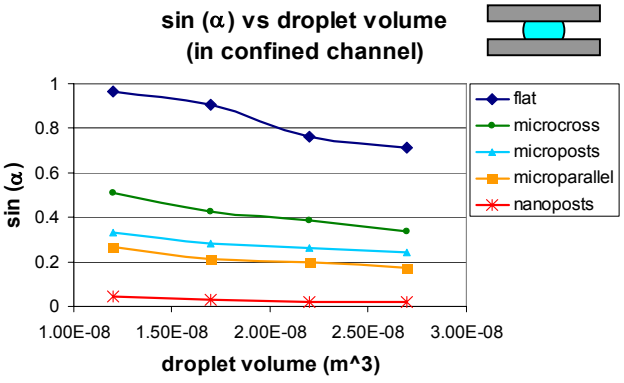

(b)

Fig. 6*: Plots of testing results. (a) on open surface and (b) in confined channel.*

tilting angle that initiates droplet rolling was so small that it could not even be measured with current testing setup ($\alpha << 1^o$). The droplet cannot be stabilized even on a well-leveled nanostructured surface.

From the results, one can see that flow resistance is affected not only by the contact angle but also by the layout patterns. First, comparing a droplet movement on microline pattern in cross direction and parallel direction, the advancing and receding side of droplet needs to overcome sequential energy barriers (jump to next line pattern over air gap) in cross direction which creates more contact angle hysteresis. Conversely, in parallel direction, energy barriers are set and kept constant along with moving direction, therefore the hysteresis is less than cross direction. Comparison of contact angle hysteresis (cross and parallel directions) can be seen in a previous study [9]. Similar explanation can be applied to micropost pattern.

The effect of different surfaces for both open and channel configuration is summarized in Table I. The results show that droplet flow resistance can be reduced, using nanostructured hydrophobic surfaces, down to less than 1% that of flat surface on open surface and less than 5% that of flat surface inside channel.

***Table I** : Flow resistance of a droplet relative to flat surface .*

	Flat surface (as reference)	microline pattern (cross direction)	microline pattern (parallel direction)	Micropost pattern	Nanopost pattern
On open surface	1	~ 0.7	~ 0.3	~ 0.4	< 0.01
In confined channel	1	~ 0.5	~ 0.3	~ 0.35	~ 0.05

CONCLUSION AND FUTURE WORK

This paper proposes and verifies that flow resistance of droplets on open surfaces as well as in microchannels can be dramatically (over 99% and over 95%, respectively) reduced by nanomechanical hydrophobic structures.

We are currently expanding the experiments to include continuous flows in closed microchannels. Low flow resistance is a critical advantage in microfluidic systems, reducing operation power for almost every application but especially hand-held devices.

ACKNOWLEDGMENTS

The authors would like to thank Prof. C. M. Ho, R. L. Garrell, F. Wudl and Mr. U. Ulmanella for their valuable discussion. This work is supported by NSF CAREER Award, NSF XYZ on Chip Program, NSF Nanoscale Interdisciplinary Research Team (NIRT) Program, and DARPA BioFlips Program. Travel support was provided by the DARPA/MTO MEMS Program.

REFERENCES

[1] S. Shibuichi, T. Onda, N. Satoh, and K. Tsujii, "Super water-repellent surfaces resulting from fractal structure," J. Phys. Chem. 100, 1996, pp. 19512-19517.

[2] M. Miwa, A. Nacajima, A. Fujishima, K. Hashimoto, and T. Watanabe, "Effects of the surface roughness on sliding angles of water droplets on superhydrophobic surfaces, Langmuir, 16,2000, pp. 5754-5760.

[3] W. Chen, A.Y. Fadeev, M. C. Hsieh, D. Öner, J. Youngblood, and T. J. McCarthy, "Ultrahydrophobic and ultralyophobic surfaces: Some comments and examples," Langmuir, 15,1999, pp. 3395-3399.

[4] A. Torkkeli, J. Saarilahti, A. Häärä, H. Härmä, T. Soukka, and P. Tolonen, "Electrostatic transportation of water droplets on superhydrophobic surfaces," MEMS '01, pp. 475-478.

[5] J. P. Youngblood and T. J. McCarthy, **"**Ultrahydrophobic polymer surfaces prepared by simultaneous ablation of polypropylene and sputtering of poly (tetrafluoroethylene) using radio frequency plasma," Macromolecules, 32, 1999, pp. 6800-6806.

[6] Y. Inoue, Y. Yoshimura, Y. Ikeda, and A. Kohno, "Ultra-hydrophobic fluorine polymer by Ar-ion bombardment," Colloids and Surfaces B, Biointerfaces, 19, (2000), pp. 257–261.

[7] Y. Matsumoto and M. Ishida, "The property of plasma-polymerized fluorocarbon film in relation to CH_4/C_4F_8 ratio and substrate temperature," Sensors and Actuators 2000, 83, pp. 179-185.

[8] A. Hozumi, and O. Takai, "Preparation of ultra water-repellent films by microwave plasma-enhanced CVD," Thin Solid Films, 303, 1997, pp. 222-225.

[9] J. Bico, C. Marzolin, and D Quéré, "Pearl drops," Europhys. Lett, 47, 1999, pp. 220-226.

[10] A. Nakejima, K. Hashimoto, and T. Watanabe, "Recent studies on super-hydrophobic films," Monatshefte für Chemie 132, 2001, pp. 31-41.

[11] A. B. D.Cassie, S. Baxter, trans. Faraday Soc., 40, 1944, pp. 546.

[12] E. Wolfarm, and R. Faust, "Wetting, spreading, and adhesion," J. F. Padday, Ed., Academic Press, London, 1978, Chapter 10.

[13] C.G.L. Furmidge, "Studies at phase interfaces, I. The sliding of liquid drops on solid surfaces and a theory for spray retention," J. Colloid Sci., 17, 1962, pp. 309-324.

[14] H. Jansen, M. de Boer, R. Legtenberg, and M. Elwenspoek, "The black silicon method: a universal method for determining the parameter setting of a fluorine-based reactive ion etcher in deep silicon trench etching with profile control," J. of Micromech. and Microeng., vol.5, (no.2), June 1995. p.115-120.

[15] H. Jansen, M. de Boer, and M. Elwenspoek, "The black silicon method VI: High aspect ratio trench etching for MEMS applications," MEMS 95, Feb. 1996, pp.250-257.